MASS-WASTING FEATURES IN VESTA'S SOUTH POLAR REGION. K. A. Otto[1] (katharina.otto@dlr.de), R. Jaumann[1, 2], K. Krohn[1], K.-D. Matz[1], F. Preusker[1], T. Roatsch[1], P. Schenk[3], F. Scholten[1], K. Stephan[1], C. A. Raymond[4] and C. T. Russell[5], [1]Deutsches Zentrum für Luft- und Raumfahrt (DLR), Institute of Planetary Research, Rutherfordstraße 2, 12555 Berlin, Germany, [2]Institute of Geosciences, Freie Universität Berlin, Berlin, Germany, [3]Lunar and Planetary Science Institute, Houston, Texas, USA, [4]California Institute of Technology, Jet Propulsion Laboratory, Pasadena, California, USA, [5]Institute of Geophysics and Planetary Physics, University of California, Los Angeles, California, USA

Introduction: The DAWN spacecraft orbited asteroid (4) Vesta from August 2011 until September 2012 [1]. The Framing Camera (FC) on board the space craft collected image data of the asteroids surface with a resolution of about 70 m/pixel in the High Altitude Mapping Orbit (HAMO) and up to 20 m/pixel in the Low Altitude Mapping Orbit (LAMO). The FC obtained multiple images of the same area with different viewing geometries in HAMO resolution. Based on this stereo data set, a three-dimensional Digital Terrain Model (DTM) has been constructed on a reference spheroid of 285 km by 229 km [2]. Vesta's southern hemisphere exhibits two large basins, Rheasilvia and underlying Veneneia [3, 4]. The region around these basins shows various types of mass-wasting features that can be correlated to the basin formation and degradation processes [5]. We used LAMO images and the DTM to identify and map six different types of mass-wasting features.

Intra-crater Mass Wasting:

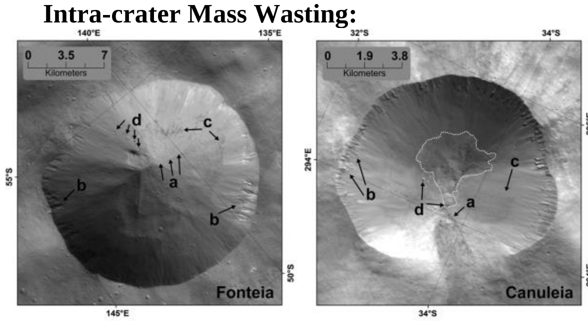

(a) (b)

We considered five intra-crater mass-wasting features. These include lobate downslope movement of debris (arrows a), spurs along the rims of the craters (arrows b), dark albedo patches overrun by brighter material (arrows c), boulders accumulated on the craters' floors and walls (arrows d), and talus material (dotted white line in (b)) [5].

The intra-crater mass-wasting features are distributed almost homogenously throughout the southern hemisphere indicating similar material properties. Older impact craters often lack fragile intra-crater mass-wasting features such as boulders, spurs and dark patches. It is likely that they have been eroded by intra-crater landslides triggered by local seismic shaking of subsequent impacts [5].

Flow-Like Features:

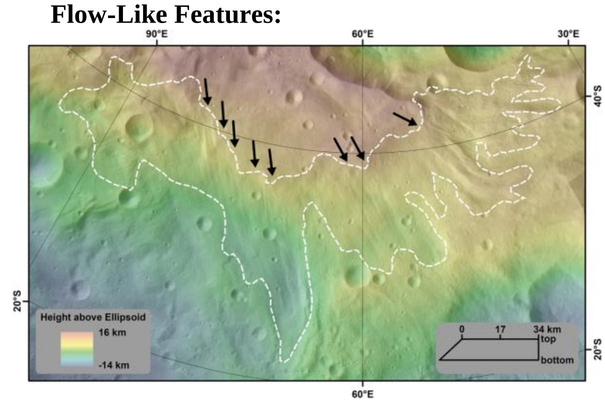

The Rheasilvia basin exhibits flow-like mass movements (dashed white line), which show a flume-like pattern with striations parallel to the direction of travel (arrows) and lobate scarps at the front of the features. The striations suggest fluid-like flow behavior, indicating that the frictional forces between the particles are small [5].

Creep-Like Features:

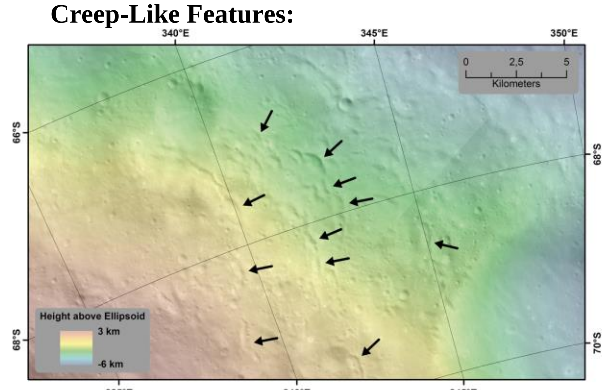

Other mass-wasting features occurring on Vesta's southern hemisphere are creep-like mounds on the regolith covered surface (arrows). These mounds are elongated features with a straight or slightly curved shape. Their lengths vary from a few hundred meters to several kilometers and they often appear in clusters with a curved alignment perpendicular to the slope [5].

Flow-like and creep-like features cluster within the region of 0°E and 90°E on the southern hemisphere. This is an area where the Rheasilvia impact ejecta has been proposed [7, 8]. It is probably that this highly shocked and fractured material exhibits properties different from the other extant surface material [5].

Slumping:

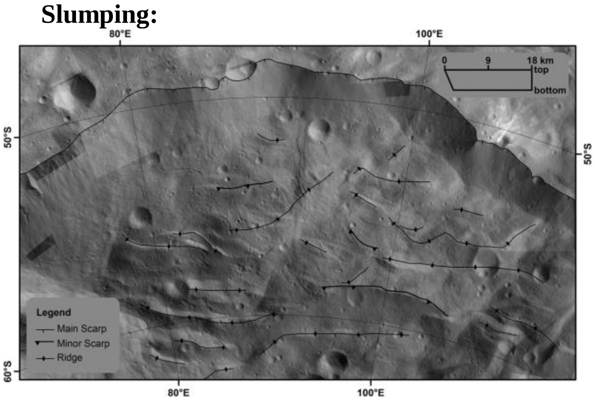

Rheasilvia has degraded due to slumping in various regions. Slumping features include almost vertical scarps, heads that are tilted backward toward the scarp, transverse cracks, ridges, and toe features at the front of the slumping bodies. A prominent and relatively young area of rotational slumping blocks appears along the Matronalia Rupes scarp toward the center of the Rheasilvia basin [5, 6].

Slides:

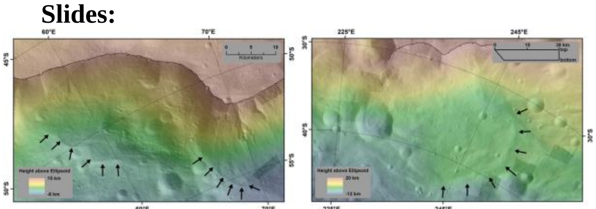

(a) (b)

The Rheasilvia basin exhibits multiple ancient and recent landslides (arrows). The less eroded and younger landslides tend to be less massive in volume and runout length. The landslides migrated from the rim and central peak of Rheasilvia toward the basin floor. For most identified slides, an eroded scarp can be observed. The resting bodies of the slides consist of elongated lobes or widened fans of material [5].

Slumping and sliding areas are mutually exclusive due to their compact and granular material properties, respectively [5].

Curved Ridges:

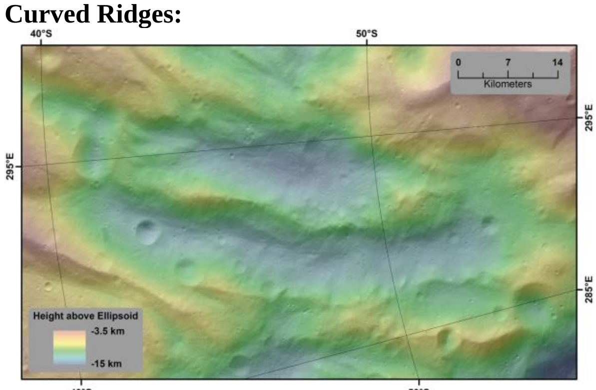

The Rheasilvia floor is characterized by numerous ridges and grooves that extend radially over the impact basin. The radial ridges are curved and up to 100 km long. They often run in parallel, with valleys separating them. In some cases, the valleys exhibit flow-like structures, indicating material migration [5].

The Rheasilvia basin also exhibits concentric ridges parallel to the crater rim. They are generally smaller than the radial ridges with lengths of up to 10 km. They often occur perpendicular to the slope which makes it likely they originated from the concentric crater collapse and relaxation after Rheasilvia had formed [5].

Conclusions: We identified six different types of mass-wasting features within the south polar region of Vesta. These features are evidence for the collapse and degradation of the Rheasilvia and Veneneia basins. Intra-crater mass wasting is present in smaller craters throughout the basins. Flow-like and creep-like features show the material behavior of highly fractured and shocked material produced by the Rheasilvia impact. Slumping and sliding are the most effective degradation processes due to their number and size. Curved radial and concentric ridges are the remnants of the early mass wasting in the modification stage of the Rheasilvia basin and the collapsed Rheasilvia wall, respectively.

References: [1] Russell et al. (2013) *Meteoritics & Planet. Sci.*, doi: 10.1111/maps.12091. [2] Preusker et al. (2012) EPSC *VII*, Abstract #EPSC2012-428-1. [3] Jaumann R. et al. (2012) *Science*, *336*, 687-690. [4] Schenk P. et al. (2012) *Science*, *336*, 694-697. [5] Otto et al. (2013) *JGR*, *118*. [6] Reddy V. et al. (2012) *Science*, *336*, 700-704. [7] De Sanctis C. et al. (2012) *Science*, *336*, 697-700. [8] Krohn et al. (2013) EGU *XV*, Abstract #EGU2013-3213.